Propulsion and Energy Forum
July 25-27, 2016, Salt Lake City, UT
52nd AIAA/SAE/ASEE Joint Propulsion Conference

Collisionless electron cooling in unmagnetized plasma thruster plumes

Mario Merino,*† Aurélien Proux‡, Pablo Fajardo† and Eduardo Ahedo§
Equipo de Propulsión Espacial y Plasmas (EP2), Universidad Carlos III de Madrid, Leganés, Spain.

A kinetic model of electrons in a steady-state, collisionless, paraxial plasma plume is presented. The model is based on the conservation of an adiabatic invariant related to the oscillating radial motion of the electrons in the electric potential of the plume. The electron phase space can be divided into distinct regions according to their connectivity with the upstream or downstream boundary conditions, and may include isolated regions of trapped electrons. A particular plasma potential is used to illustrate the capabilities of the model. This electron model is the first and fundamental piece of a full plasma plume model that will allow the self-consistent computation of the ion, electron, and electric potential responses in order to investigate electron collisionless cooling mechanisms in an unmagnetized plasma plume.

I. Introduction

The expansion of plasma plumes produced by electric propulsion systems in space has been a topic of active research for several years.[1,2] The common goal of these studies is to understand how ions, neutrals and electrons behave and to characterize their interaction with the spacecraft, a major concern for systems integrators as the plasma can erode and contaminate delicate surfaces, affect the electric potential around the spacecraft, induce electric discharges at the interconnectors of solar cells, and interfere with telecommunications and optical sensors.[3–7] Novel electric propulsion applications, such as the contactless deorbiting of space debris or the repositioning of asteroids with plasma plumes, as in the ion beam shepherd concept,[8,9] is also concerned about the interaction of the plasma with a downstream object immersed in it.

Plasma plumes of different thrusters (e.g. Hall effect thrusters[10–16] and gridded ion thrusters[17–21]) are routinely characterized in detail in laboratory experiments using plasma probes and optical diagnostics. These experiments can faithfully recover the properties of the primary ions created inside the plasma thruster. For instance, Faraday cups and retarding potential analyzers are commonly used to obtain the ion current and ion energy distribution functions at distances of about 1 m from the thruster exit. However, the properties of secondary ions (i.e., those generated outside of the thruster by charge-exchange collisions with neutrals or by ionization), which can play a major role in the plasma-spacecraft interaction problem since they are accelerated at large angles from the centerline by the electric field, are harder to assess in the vacuum chamber. This is due to several factors that affect laboratory experiments and make them not fully representative of the operational conditions in space: firstly, the background pressure in the vacuum chambers is usually several orders of magnitude larger than at low Earth orbit.[22] As a direct consequence, a much larger number of charge-exchange ions is produced in the laboratory than in space, as evidenced by the few existing in-space measurements of electric propulsion plasma plumes.[6,12,23–26] Secondly, and more subtle, the set-up of the electric potential that controls the motion of the slow secondary ions is dominantly affected by the electron response in the plume. As the electron motion in the plume is nearly collisonless and most of the electron cloud is effectively confined by the electric field, their response has a *global* character and is influenced by the presence of the (conductive) chamber walls, the operating point of the neutralizer, and the details of the electrical connection of the neutralizer and thruster to ground, problems that were

*Contact: mario.merino@uc3m.es.
†Assistant Professor, Aerospace Engineering Department, Avda. de la Universidad 30, 28911 Leganés (Madrid) Spain.
‡Exchange MSc student (ENSTA-Paristech).
§Full Professor, Aerospace Engineering Department, Avda. de la Universidad 30, 28911 Leganés (Madrid) Spain.

already pointed out by Korsun et al.[6] In particular, the local electron temperature dictates the magnitude of the potential fall in the plume, of major importance in all plume/spacecraft interaction studies.

Naturally, the determination of plasma properties in the plume has also been approached by modeling and numerical simulation. The plume can be generally divided into two regions, each with different simulation requirements: in the near-region, residual electric and magnetic fields from the thruster, the presence of the neutralizer, and collisional effects are important. This makes the near-region a difficult problem hard to model in simplified ways. In the far-region (typically starting a few thruster radii downstream), the plasma profiles are smooth, collisions and thruster fields are negligible, and the expansion is governed fundamentally by ion inertia and the residual electron pressure. The far-region is therefore more amenable to simple models.

Common modeling approaches range from single- and many-fluid models to particle-in-cell (PIC) and hybrid PIC/fluid models. Fluid models are characterized by their simplicity and cleanness in their solution, but also by the limited physics that can sensibly be included in them. Additionally, they require an external closure relation for the each species equations; this relation typically prescribes temperature or the heat flux in the species as a function of lower moments of the distribution function (e.g. density). Examples of fluid models based on the continuity and momentum equation of each species that assume cold ions and impose the closure at the electron temperature level include self-similar models,[27–29] and the EASYPLUME code.[30] The closure electron models used are based on the isothermality assumption, $T_e = T_{e0} = \text{const}$, or polytropic cooling laws, $T_e \propto n_e^{\gamma-1}$, where T_e, n are the electron temperature and density, and γ is a number that is typically chosen to fit existing experimental or fully-numerical results,[16,31] frequently ranging between 1 and 1.3.

Particle-based approaches, on the contrary, require larger computation resources but are very adequate for studying the different sub-populations of ions and neutrals. The inherent numerical noise associated with PIC simulations is a major issue that restricts the accuracy that is attained with these models. The tremendous computational cost makes full-PIC models impractical to simulate plasma plumes over the large distances and times of interest, and their usage is restricted to a few specific studies.[32,33] In contrast, in hybrid PIC/fluid models heavy species are modeled as particles and electrons are modeled as one or more fluids. Additionally, most hybrid models invoke quasineutrality to compute the electric field in the plume, an assumption that is satisfactorily fulfilled in all but specific problems. These two choices are advantageous from a computational point of view, as they relax considerably the constraints on the maximum simulation timestep and cell size for numerical stability. However, the use of electron fluid models requires again an external closure relation. The same options exist as with fully-fluid models; in particular, the near-totality of existing codes relies on isothermal and polytropic electron models. Examples of hybrid codes thus constructed include the code of Ref. 34, the AQUILA code,[35] the COLLISEUM/DRACO code[36] (or its new version, SM/MURF[37]), SPIS,[38] and EP2PLUS.[39]

A major limitation of the simple fluid closure relations for electrons described above and used in both fully-fluid and hybrid PIC/fluid plasma plume models is that they are not strictly satisfied in the collisionless plasma plume. While similar relations are easy to justify in collisional gases that satisfy the local thermodynamic equilibrium (LTE) condition, plume electrons are far from LTE and indeed the consistent electron distribution function must be determined globally. This lack of physical justification has been tolerated to some extent as these simple models can be approximately adjusted to experimental results after some tuning (with parameters such as T_{e0} and γ). However, this approach provides no insight on electron dynamics and cooling mechanisms in the collisionless plume, which dictate the electric potential fall along it and the secondary ion solution, and gives no clues as to the "translation" of laboratory experiments into space conditions.

In order to correctly solve the complex electron global response, a kinetic approach seems unavoidable. Luckily, the plasma plumes of electric thrusters (in particular, their far-region) present several advantageous characteristics, such as axisymmetry and moderate divergence, that can be exploited to set up a nearly-analytical kinetic model. In a previous study,[40,41] a steady-state 1D-2V kinetic model based on the conservation of energy and the quasi-conservation of the magnetic moment of each electron in a strong convergent-divergent magnetic field (i.e., a magnetic nozzle[42,43]), which improved on a previous non-stationary model by Arefiev and Breizman,[44] was established and used to compute the evolution of electron temperature in the collisionless plasma and derive simple closure relations that can be used to inform fluid electron models. The success of that model for a similar, related problem encourages us to follow a similar approach for the case of interest here (an unmagnetized plasma plume). However, this requires finding first an alternative adiabatic invariant that plays the role of the magnetic moment in a magnetized plasma plume. Such invariant must

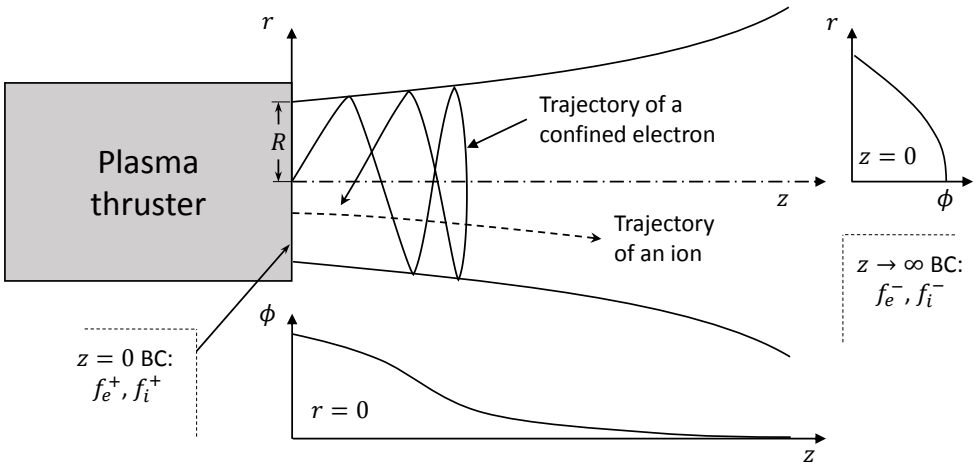

Figure 1. Sketch of the collisionless, paraxial plasma plume expansion problem. Ions and electrons are generated in a plasma source and injected into the domain at $z = 0$. The electric potential ϕ is assumed to be monotonically decreasing in the axial and radial directions. This potential accelerates ions downstream and confines most of the electron cloud. Example electron and ion trajectories are sketched in the figure; electrons typically bounce several times in the radial direction due to the confining potential before turning around. The boundary conditions (BC) are f_i^+, f_e^+ at $z = 0$, the ion and electron distribution functions in the semispace $v_z > 0$, and f_i^-, f_e^- at $z \to \infty$, the distribution functions with $v_z < 0$.

describe the radial motion of electrons in the monotonically decreasing electric potential of the plume. A first proposal of such invariant, in a different problem, was advanced by Martínez-Sánchez.[45] Moreover, the fully-2D character of the unmagnetized plume expansion the expansion has to be taken into account, a fact that differs from the 1D approach that is possible in fully-magnetized plasmas.

The present work establishes a 2D-3V kinetic model of an axisymmetric, paraxial collisionless electron plume based on the quasi-conservation of an action integral that is one of the adiabatic invariants of the electron motion. The validity and limitations of this model are discussed. This model represents the first (and major) part of a complete self-consistent plasma plume model that shall include ions and the iterative computation of the plasma electric potential; the characteristics and the solution algorithm of the complete model are commented on. Preliminary results of the electron response in a prescribed but representative electric potential are presented and discussed.

The rest of the paper is organized as follows: Section II presents the electron model and discusses its validity and limitations. Section III contains preliminary results of the electron solution in a fixed, radially-parabolic electric potential. The discussion of the full plasma plume model integrating ions and solving iteratively for the electric potential can be found in Section IV. Finally, Section V gathers the first conclusions of this ongoing work and discusses next steps.

II. Electron model formulation

Consider an ion-electron plasma that expands from a source through a circular aperture of radius R at $z = 0$ into vacuum ($z > 0$), as depicted in Figure 1. The plasma source is electrically floating with respect to infinity.

The plasma expansion will be assumed collisionless, quasineutral, axisymmetric, non-rotating, globally-current-free, and paraxial. This last assumption means that axial variations of all plasma variables are much smaller than radial variations, according to the following ordering:

$$R\frac{\partial}{\partial z} \sim \varepsilon, \tag{1}$$

with $\varepsilon \ll 1$. These conditions represent satisfactorily most of the far-region plasma plumes of electric propulsion devices.

The distribution function of each species is decomposed as $f_i = f_i^+ + f_i^-$ and $f_e = f_e^+ + f_e^-$, separating the

particles traveling downstream ($v_z > 0$, positive sign) and upstream ($v_z < 0$, negative sign). The boundary conditions of the problem are f_i^+ and f_e^+ at the source exit ($z = 0$) and f_i^- and f_e^- at infinity downstream ($z \to \infty$). For an expansion into perfect vacuum, $f_i^- = f_e^- = 0$ there.

The ultimate objective of the full model is to solve the ion and electron distribution functions, f_i and f_e, self-consistently with the plume electric potential ϕ, in $z > 0$. The present electron model strives to solve f_e in a prescribed electric potential, as a first step toward that goal. We shall only focus on plume expansions where the plasma potential ϕ satisfies:

$$\partial\phi/\partial r \leq 0; \quad \partial^2\phi/\partial r^2 \leq 0. \tag{2}$$

Additionally, it is assumed that ϕ is sufficiently negative as $r \to \infty$ to prevent electrons of all energies in the range of study from escaping radially. Under these conditions, most electrons are confined radially and axially and their trajectories bounce off repeatedly at the sides of the plume, whereas all ions are simply accelerated outward.

A. Motion of a single electron in a paraxial electric potential

The Hamiltonian $\mathcal{H}$ of an electron of mass m_e and charge $-e$ in a stationary electric potential $\phi(z, r)$ in cylindrical variables $(z, r, \theta, v_z, v_r, v_\theta)$ is given by

$$\mathcal{H}(z, r, p_z, p_r, p_\theta) = \frac{1}{2m_e}\left(p_z^2 + p_r^2 + \frac{p_\theta^2}{r^2}\right) - e\phi(z, r), \tag{3}$$

where the canonical momenta are defined as $p_z = m_e v_z$, $p_r = m_e v_r$, and $p_\theta = m_e r v_\theta$.

Since $\mathcal{H}$ does not depend explicitly on time t, $\mathcal{H}$ is a first conserved quantity of motion and it coincides with the mechanical energy of the electron, E. Furthermore, as θ is a cyclic variable, the angular momentum about the axis, p_θ, is a second conserved quantity of the problem. Our goal is to find a third conserved quantity, so that the motion of the particle can be reduced to three conservation laws.

1. *Topology of phase space*

If we treat E, p_θ as constant parameters of the motion of the electron, the effective phase space is 4-dimensional: z, r, p_z, p_r. The mathematical constraint

$$\mathcal{H}(z, r, p_z, p_r; p_\theta) = E \tag{4}$$

defines a 3-dimensional manifold $\mathcal{V}_E$ in this phase space, which represents the states in which an electron with energy E and angular momentum about the axis p_θ can exist. The manifold $\mathcal{V}_E$ is symmetric about $p_z = 0$ and $p_r = 0$, and is even in r.

Let Γ_0 be the curve that results from the restriction of $\mathcal{V}_E$ to $\{z = z_0; p_z = p_{z0}\}$, i.e., its intersection with a given (r, p_r) plane. Under the conditions imposed on ϕ in Eq. (2), the potential is electron-confining in the radial direction and the curve Γ_0 is a single closed loop.

If we treat each point in Γ_0 as the initial position of a virtual electron and we propagate its trajectory according to the Hamiltonian equations of motion, a 2-dimensional surface Σ_0 in the 4 dimensional phase space results, which is embedded in $\mathcal{V}_E$.

2. *Separable potential*

When $\phi(z, r)$ is separable as $\phi(z, r) = \phi_z(z) + \phi_r(r)$, we can write the Hamiltonian as

$$\mathcal{H}(z, r, p_z, p_r; p_\theta) = \mathcal{H}_z(z, p_z) + \mathcal{H}_r(r, p_r; p_\theta) \tag{5}$$

where

$$\mathcal{H}_z(z, p_z) = \frac{p_z^2}{2m_e} - e\phi_z(z) = E_z; \quad \mathcal{H}_r(r, p_r; p_\theta) = \frac{1}{2m_e}\left(p_r^2 + \frac{p_\theta^2}{r^2}\right) - e\phi_r(r) = E_{r\theta} \tag{6}$$

and $E_z, E_{r\theta}$ are each conserved independently. In this case, the surface Σ_0 can also be defined as the 2-dimensional manifold that satisfies the equations $E_z = \text{const}$ and $E_{r\theta} = \text{const}$.

On the surface Σ_0 we can define the following differential 1-form and its integral along Γ_0,

$$\omega_{r1} = p_r dr; \quad J_{r0} = \int_{\Gamma_0} \omega_{r1}. \tag{7}$$

As a consequence of the separability of $\mathcal{H}$, ω_{r1} is *exact* over Σ_0. This means that the integral of ω_{r1} along a closed path Γ embedded in Σ_0 does not depend on the details of the path itself, but rather on its topological class (i.e., whether it is smoothly reducible to a point, whether it winds once or more times around Σ_0, etc). In particular, the integral of ω_{r1} along Γ_0, which winds once about Σ_0 in the r, p_r plane, or along any topologically-equivalent curve, coincides with the *action integral* J_r associated to the r motion of the electron,

$$J_{r0} \equiv J_r = \oint \omega_{r1} = 2\int_{r_{\min}}^{r_{\max}} \mathrm{d}r \sqrt{2m_e \left(E_{r\theta} + e\phi_r\left(r\right)\right) - \frac{p_\theta^2}{r^2}}, \tag{8}$$

where, $r_{\min}$ and $r_{\max}$ are the limits of the motion of the particle in the r direction. Note that, as all action integrals, the units of J_r are those of angular momentum. The integral J_r is a property of the surface Σ_0 itself, and therefore, this is a third conserved quantity of motion that we can use to describe the problem conveniently (together with E and p_θ). Obviously, E_z and $E_{r\theta}$ would be alternative candidates to E and J_r carrying the same information. However, using J_r (more precisely, J_{r0}) has several advantages when the potential is not strictly separable, as will be shown below.

To complete the description of the radial motion of a single electron, it is convenient to introduce a phase angle variable β_r that grows linearly in time,

$$\beta_r(r) = \int \frac{\partial}{\partial J_r} p_r\left(r, J_r; p_\theta\right) \left|\mathrm{d}r\right|. \tag{9}$$

where p_r needs to be expressed as a function of r and J_r before taking the derivative, and the notation $|\mathrm{d}r|$ is used to indicate that the sign of the integrand should be changed for the part of the trajectory of the electron where $p_r < 0$. This equation can be used to relate r with β_r. Observe that β_r is incremented in one unit every full radial orbit of the electron. In this way, $\beta_r = k$ at $r = r_{\min}$ and $\beta_r = k + 1/2$ at $r = r_{\max}$, with $k \in \mathbb{Z}$. The variables β_r, J_r are canonical conjugated variables that can be used to define a canonical transformation of phase space where the new variables are z, β_r, p_z, J_r.

3. Non-separable paraxial potential

In a plasma plume, the electric potential is usually non-separable. While the following derivation is applicable to more general potentials, we shall now assume that we can write $\phi\left(z, r\right)$ as

$$\phi(z, r) = \phi_0\left(\frac{r}{h\left(\varepsilon z\right)}\right) + \phi_1(\varepsilon z) + O(\varepsilon^2 z) \tag{10}$$

where ε is the small parameter that describes the relative magnitude of axial variations in the paraxial plume, as discussed above; the nondimensional function h represents the gradual "opening" of the plasma jet due to its divergence angle, with $h\left(0\right) = 1$; and ϕ_1 is the axial potential fall along the plume. We arbitrarily impose $\phi_0(0) = \phi_1\left(0\right) = 0$. This form of the potential is consistent with that found in self-similar fluid models, which have been shown to satisfactorily approximate actual plasma plumes,[30] and according to this definition, any non-self-similar feature of the electric potential is assumed to be of order ε^2. Note that a paraxial potential such as this one is separable at order zero in ε, but it is not separable at higher orders.

In a general non-separable potential ω_{r1} is not an exact 1-form, and E_z, $E_{r\theta}$ are not cleanly defined as above; in fact, there can exist an energy transfer from the r, θ directions to the z direction, something that did not occur in the separable case. Observe that, while the action integral J_r is no longer equal to J_{r0} in general since the path of integration now matters, J_{r0} is still well defined at any $z = z_0$ and $p_z = p_{z0}$, and can be used as a phase space coordinate to study the electron motion,

$$J_{r0}(z_0, p_{z0}; E, p_\theta) = 2\int_{r_{\min}}^{r_{max}} \mathrm{d}r \sqrt{2m_e\left(E - \frac{p_{z0}^2}{2m_e} + e\phi\left(z_0, r\right)\right) - \frac{p_\theta^2}{r^2}}, \tag{11}$$

where z_0 and p_{z0} have to be considered constant in the integral. Note that, in contrast to J_{r0} which is defined along Γ_0, the action variable J_r must be defined along an actual particle trajectory for a full r cycle, a path along which z, p_z can change (and which does not close on itself in general).

Nevertheless and strictly, the integral J_{r0} is *not* a constant of the motion of the electron in the general potential case. Its time variation along the motion of a particle is given by

$$\frac{\mathrm{d}J_{r0}}{\mathrm{d}t} = \frac{\partial J_{r0}}{\partial z_0}\frac{p_{z0}}{m_e} + e\frac{\partial J_{r0}}{\partial p_{z0}}\frac{\partial \phi\left(z_0, r_0\right)}{\partial z_0} = 2ep_{z0}\int_{r_{\min}}^{r_{\max}} \frac{\partial\phi(z_0,r)/\partial z_0 - \partial\phi(z_0,r_0)/\partial z_0}{\sqrt{2m_e\left(E - \dfrac{p_{z0}^2}{2m_e} + e\phi\left(z_0,r\right)\right) - \dfrac{p_\theta^2}{r^2}}}\mathrm{d}r, \tag{12}$$

where z_0, r_0 and p_{z0} have to be considered constant in the integral. Clearly, the integral is in general non-zero. Observe that in the separable case the numerator of the integrand vanishes and $dJ_{r0}/dt = 0$ (confirming that $J_{r0} \equiv J_r$ is a conserved quantity of the electron motion under those conditions).

The derivative of ϕ in the z direction is of order ε according to the paraxiality assumption, and, moreover, its second derivative goes as ε^2. Inspecting Eq. (12), the fact that $\partial\phi/\partial z \sim \varepsilon$ means that $\mathrm{d}J_{r0}/\mathrm{d}t \sim \varepsilon$, too.

Interestingly, the *average* change of J_{r0} over half a period $\tau/2$ of the r motion of an electron vanishes to order ε. This can be proven by integrating $\mathrm{d}J_{r0}/\mathrm{d}r$ in time along the trajectory $z_0(t), r_0(t), p_{z0}(t), p_{r0}(t)$ of a particle,

$$\int_0^{\tau/2}\frac{\mathrm{d}J_{r0}}{\mathrm{d}t}\mathrm{d}t = \int_{r_{0\,\min}}^{r_{0\,\max}}\frac{\mathrm{d}J_{r0}}{\mathrm{d}t}\frac{m_e\mathrm{d}r_0}{\sqrt{2m_e\left(E - \dfrac{p_{z0}^2}{2m_e} + e\phi\left(z_0,r_0\right)\right) - \dfrac{p_\theta^2}{r_0^2}}} =$$

$$= \int_{r_{0\,\min}}^{r_{0\,\max}}\mathrm{d}r_0\int_{r_{\min}}^{r_{\max}}\mathrm{d}r\frac{2em_ep_{z0}\left[\partial\phi\left(z_0,r\right)/\partial z_0 - \partial\phi\left(z_0,r_0\right)/\partial z_0\right]}{\sqrt{2m_e\left(E - \dfrac{p_{z0}^2}{2m_e} + e\phi\left(z_0,r_0\right)\right) - \dfrac{p_\theta^2}{r_0^2}}\sqrt{2m_e\left(E - \dfrac{p_{z0}^2}{2m_e} + e\phi\left(z_0,r\right)\right) - \dfrac{p_\theta^2}{r^2}}}, \tag{13}$$

where z_0, p_{z0}, $r_{\min}$ and $r_{\max}$ have to be considered functions of r_0, the variable that has been used to parametrize the particle trajectory in the last two expressions. We note that during the half-orbit: (i) the variation of $r_{\min}$, $r_{\max}$ is at most of order ε, (ii) the variation of p_{z0} is of order ε, but (iii) z_0 can change in order $O\left(1\right)$. Clearly, for the extent of the half-orbit, $\partial\phi/\partial z$ is to order ε only a function of r:

$$\frac{\partial\phi}{\partial z}\left(z,r\right) = \varepsilon A\left(r\right) + O\left(\varepsilon^2\right), \tag{14}$$

Therefore we can rewrite the bracket inside the numerator of the integrand of Eq. (13) as

$$\varepsilon\left[A(r) - A(r_0)\right] + O\left(\varepsilon^2\right), \tag{15}$$

and the ε-order integral cancels out exactly due to the symmetry of the integration domain. As a consequence, J_{r0} *does not have any secular term of order* ε along the motion of the particles, but only a periodic component that depends on the motion along the radial orbit. This result is analogous to the well-known quasi-invariance of action integrals in separable, conservative problems when the Hamiltonian is perturbed in time,[46] and encourages us to use E, p_θ and J_{r0} to describe the motion of the electrons.

Regarding the definition of the radial phase angle β_r in the non-separable paraxial case, for consistency, we shall maintain the definition of β_r given above considering fixed values of $z = z_0$, $p_z = p_{z0}$ and $J_r = J_{r0}$, and call it β_{r0}. Note that, strictly speaking, β_{r0} is not the true phase angle as defined in the spirit of action-angle variables, and that this approximation incurs in a small difference of order ε. However, in spite of the fact that the coordinates J_{r0} and β_{r0} so defined are no longer canonically conjugated variables, they can still be used as valid coordinates to label the state of an electron in phase space.

B. Evolution of the distribution function of a collisionless electron species

We now turn our attention to the collisionless evolution of the distribution function f_e of an electron species moving in a paraxial potential ϕ in the form given in Eq. (10). We note that in an axisymmetric plume, f_e in velocity phase space $(z, r, \theta, v_z, v_r, v_\theta)$ will be symmetric in r and v_r at the axis $(r = 0)$, and it must be uniform in θ. In the particular case of a non-rotating plume f_e is also assumed to be symmetric in v_θ for all r.

Apart from the usual velocity-based phase space already defined, we shall define an "energy-based" phase space $(z, \beta_{r0}, \theta, E, J_{r0}, p_\theta)$ where J_{r0} is the action-like integral defined in Eq. (11) and β_{r0} is the angle-like

variable defined above. This new set of parameters is not canonical in the sense of Hamilton unless the problem is separable, but is still a valid set of coordinates to describe the particle phase space. Note that, since in this energy-based space it is not possible to distinguish electrons with $p_z > 0$ and $p_z < 0$, it is convenient to decompose f_e into $f_e = f_e^+ + f_e^-$, where each summand represents the population of electrons traveling to downstream and upstream, as defined before. In the energy space, the total derivative of f_e along the particle motion, given by Vlasov's equation, can be written as

$$\frac{\mathrm{d}f_e}{\mathrm{d}t} = \frac{\partial f_e}{\partial t} + v_z \frac{\partial f_e}{\partial z} + \dot{\beta}_{r0} \frac{\partial f_e}{\partial \beta_{r0}} + v_\theta \frac{\partial f_e}{\partial \theta} + \dot{E} \frac{\partial f_e}{\partial E} + \dot{J}_{r0} \frac{\partial f_e}{\partial J_{r0}} + \dot{p}_\theta \frac{\partial f_e}{\partial p_\theta} = 0. \tag{16}$$

In steady-state, the first term on the right hand side is zero. Axisymmetry tells us that the fourth term is zero as well. The conservation of energy E and angular momentum p_θ indicate that the fifth and seventh terms are also zero.

Next, we shall make the additional assumption that f_e is uniform to order ε in the angle variable β_{r0}. This is indeed true for a confined population in steady state in the separable problem if the oscillation frequencies in the z and r directions are non-commensurate. Since the second term has $\partial f_e/\partial z = O(\varepsilon)$ due to the paraxiality assumption, and the sixth term is also $O(\varepsilon)$ due to $\dot{J}_{r0} = O(\varepsilon)$, a variation of f_e with β_{r0} of order ε may exist in the non-separable case. According to this, f_e can be written as the sum of its β_{r0}-average value (denoted with an overline) plus a β_{r0}-dependent variation that is null in average over an orbit (denoted with a hat):

$$f_e\left(z, \beta_{r0}, E, J_{r0}, p_\theta\right) = \overline{f}_e\left(z, E, J_{r0}, p_\theta\right) + \varepsilon \hat{f}_e\left(z, \beta_{r0}, E, J_{r0}, p_\theta\right), \tag{17}$$

i.e., where

$$\int_{\beta_{r0}}^{\beta_{r0}+1} f_e \mathrm{d}\beta_{r0} = \overline{f}_e; \quad \text{and} \int_{\beta_{r0}}^{\beta_{r0}+1} \hat{f}_e \mathrm{d}\beta_{r0} = 0. \tag{18}$$

Lastly, according to the discussion in the previous subsection, while the variations of J_{r0} in one r-orbit can be of order ε, the r-orbit averaged variation (i.e., the secular change) is only of order ε^2. With these considerations in mind, if we take the β_{r0}-average of Eq. (16) and keep the terms up to order ε, the evolution of $\overline{f}_e$ is given by

$$v_z \frac{\partial \overline{f}_e}{\partial z} + O\left(\varepsilon^2\right) = 0. \tag{19}$$

This result indicates that, to an accuracy of order ε, the evolution of the radially-averaged distribution function $\overline{f}_e$ is given by its constant propagation in the z direction (which are the characteristic lines of the ε-order problem). This propagation is limited by the surface $v_z\left(z, E, J_{r0}, p_\theta\right) = 0$, which describes the turning points of the electrons in the domain. The equation of the $v_z = 0$ surface can be obtained from the β_{r0}-averaged Hamiltonian $\mathcal{H}$. At every $z = \text{const}$ in the energy-based phase space, this surface is a cone with vertex at $E = J_{r0} = p_\theta = 0$ and axis coincident with the E axis.

The reflection of the electrons at this surface is due to two competing phenomena:

- On the one hand, electrostatic confinement decelerates the electrons axially, preventing all but the most energetic ones from reaching infinity downstream. Incidentally, the escaping electrons are those that maintain the global current-free condition in the plasma plume.
- On the other hand, the conservation of p_θ and the (quasi-)conservation of J_{r0}, act as adiabatic invariants. Just like the quasi-conservation of the magnetic moment in a magnetized plasma (which sets-up the magnetic mirror effect), the net effect of these conservations is that electrons with p_θ and/or $J_{r0} \neq 0$ are accelerated downstream, in the direction of broadening of the plume.

These two effects lead to an interesting decomposition of phase space according to the connectivity of electrons of a given E, J_{r0}, p_θ with the domain boundaries $z = 0$ and $z = \infty$. The following different electron subpopulations or phase space regions can be identified:

- Free electron regions, which connect to both $z = 0$ and $z = \infty$. These electrons never intersect the $v_z = 0$ surface.
- Reflected electron regions, which connect to $z = 0$ and are reflected back at some point when they reach the turning surface.

- Similar to this last group, another group exists of electrons connected to $z = \infty$, but not with $z = 0$. This region is empty, unless background electrons are injected from infinity downstream.
- Doubly-trapped electron regions, which do not connect with either $z = 0$ or $z = \infty$, but instead are doubly-limited by the surface $v_z = 0$.
- Forbidden regions, where electrons of a given E, J_{r0}, p_θ do not exist.

According to this subdivision, a simple algorithm to determine $\overline{f}_e$ in the whole domain for a given paraxial electric potential $\phi(z, r)$ can be established based on the direct method of characteristics, once the boundary conditions for $\overline{f}_e^+$ at $z = 0$ and for f_e^- at $z = \infty$ for all E, J_{r0}, p_θ are known.

1. First, compute the β_{r0} averages $\overline{f}_e^+$ at $z = 0$ and $\overline{f}_e^-$ at $z \to \infty$. For most practical cases of interest, $\overline{f}_e^+ = f_e^+$ at $z = 0$ (as $\hat{f}_e^+ = 0$ at $z = 0$). Also, if expanding into a perfect vacuum, $\overline{f}_e^- = f_e^- = 0$ at $z = \infty$.
2. We determine the surface $v_z\left(z, E, J_{r0}, p_\theta\right) = 0$ for the given ϕ using the expression of the β_{r0}-averaged Hamiltonian up to order ε. This surface delimits the regions of existence of the solution, as classified above.
3. For each E, J_{r0}, p_θ, the function $\overline{f}_e^+$ is propagated as a constant toward the right along straight z lines from $z = 0$ while $v_z > 0$. Same for $\overline{f}_e^-$ toward the left from $z \to \infty$ while $v_z < 0$:
   (a) Those z-propagation lines that do not intersect the $v_z = 0$ surface connect $z = 0$ with $z = \infty$ (free electrons).
   (b) Those z-propagation lines that connect to one end of the domain and intersect the $v_z = 0$ surface are associated to reflected particles of either type. On those lines, reflection means that $\overline{f}_e^- = \overline{f}_e^+$.
   (c) For those regions of the energy-based phase space enclosed by the $v_z = 0$ surface and unaccessible from either boundary of the domain, arbitrary values of $\overline{f}_e$ for each E, J_{r0}, p_θ are possible, with the sole condition being $\overline{f}_e^- = \overline{f}_e^+$.

Alternatively, if one is interested only in the value of $\overline{f}_e$ at one z position, the inverse method of characteristics could be used, i.e., checking for the connectivity of that z position with the boundary conditions and the $v_z = 0$ surface, for each E, J_{r0}, p_θ.

Observe that, while it is possible to compute $\overline{f}_e$ with a residual of order ε^2 by solving the simple procedure detailed above, the obtention of $\hat{f}_e$, which contains the ε-order correction of f_e in the radial direction, is far more complex than that of $\overline{f}_e$, as it would require solving the ε-order problem of the non-averaged Vlasov equation, Eq. (16). In summary, with the model formulated here it is possible obtain results that are accurate to order ε in the axial direction, but only zeroth-order in the radial direction. Fortunately, as stated above, $\hat{f}_e$ is expected to be negligible (or even zero) in many cases of interest (especially if the boundary conditions satisfy $\hat{f}_e = 0$).

Naturally, the question arises of what should be the value of $\overline{f}_e$ in the doubly-trapped regions of phase space, not connected with the boundary conditions. Clearly, the described approach cannot provide information on this. Adding a non-zero collisionality to the model, considering higher-order terms of the ε expansion, and/or solving the initial transient of the plume expansion[44] are likely required to have a fully consistent description of these regions. A time-dependent kinetic model is being developed for the magnetic nozzle problem, which may shed some light on this topic. In the absence of a better criterion at present, and following the choice taken in Ref. 40, 41, it can be assumed that after sufficiently long periods of time these regions are populated by the same distribution function as the plasma source electrons (or, alternatively a fixed fraction density of it to study the effect of these regions being only partially filled).

To conclude this section, some comments about the limits of validity of the present kinetic model of the electron population are due:

- Firstly, the expansion in ε in the model is not uniformly valid in all velocity space. Regardless of how paraxial the problem is, i.e., how small ε is, particles with $\varepsilon v_z / v_r \sim 1$ are problematic from the viewpoint of the average conservation of J_{r0}. This affects a small cone of particles in velocity-based phase space.

- Secondly, the expansion in ε may be non-uniform as $z \to \infty$ and/or as $t \to \infty$; higher-order errors may accumulate with time and as the particle travels in z.
- Lastly, related to this, the expansion used in Eq. (16) could break down near the turning surface, as $v_z \to 0$, since the ordering used to simplify the equation may be invalid in those regions.

In particular, these last two points could be related with higher-order mechanisms that could enable the access to the doubly-trapped regions from the boundary-connected regions commented above.

C. Computation of the electron distribution function moments

Once $\overline{f}_e$ is known, it is possible to compute any moment of the distribution function at any point (z, r) by direct integration. This integration can be carried out in velocity-based phase space, after transforming our solution back to it, or directly in energy-based phase space, after rewriting the corresponding integrand in energy variables.

Regardless of which phase space is used to perform the electron integrations, the transformation equations between $(z, r, \theta, v_z, v_r, v_\theta)$ and $(z, \beta_{r0}, \theta, E, J_{r0}, p_\theta)$ are required to compute the moments. The following relations, which will depend on the particular form of the electric potential, need to be used:

$$\begin{aligned} r &= r(z, \beta_{r0}, E, J_{r0}, p_\theta), \\ v_z &= v_z\left(z, E, J_{r0}, p_\theta\right), \\ v_r &= v_r\left(z, \beta_{r0}, E, J_{r0}, p_\theta\right), \\ v_\theta &= p_\theta / \left(mr\right), \end{aligned} \tag{20}$$

where r must be taken as a function of $(z, \beta_{r0}, E, J_{r0}, p_\theta)$ in the last expression too.

The expression of an arbitrary moment at (z, r) in velocity-based or energy-based phase space is then:

$$\begin{aligned} \mathcal{M}_{jk\ldots l}(z, r) &= \iiint v_j v_k \ldots v_l f_e \mathrm{d}v_z \mathrm{d}v_r \mathrm{d}v_\theta \\ &= \iiint v_j v_k \ldots v_l \left[\overline{f}_e^{+} + \overline{f}_e^{-} + \varepsilon\left(\hat{f}_e^{+} + \hat{f}_e^{-}\right)\right] |\mathcal{J}| \, \mathrm{d}E \mathrm{d}J_{r0} \mathrm{d}p_\theta \end{aligned} \tag{21}$$

where the limits of integration in the first expression are $[-\infty, \infty]$ in each velocity, and in the second expression are $E = [0, \infty]$, $J_{r0} = [0, \infty]$, and $p_\theta = [-\infty, \infty]$. Naturally, in the integrals of the second expression, $v_j v_k \ldots v_l$ have to be expressed in terms of $z, \beta_{r0}, E, J_{r0}, p_\theta$ using the relations above. Observe that the relation between β_{r0} and r must be used implicitly in the integration. Note that in a non-rotating plume, the $p_\theta = [-\infty, 0]$ and $p_\theta = [0, \infty]$ parts of the second integral are equal or cancel out due to symmetry considerations, depending on the parity of v_θ in the integrand. Finally, $|\mathcal{J}|$ is the determinant of the Jacobian matrix of the transformation:

$$\mathcal{J}\left(z, \beta_{r0}, E, J_{r0}, p_\theta\right) = \begin{bmatrix} \partial v_z/\partial E & \partial v_z/\partial J_{r0} & \partial v_z/\partial p_\theta \\ \partial v_r/\partial E & \partial v_r/\partial J_{r0} & \partial v_r/\partial p_\theta \\ \partial v_\theta/\partial E & \partial v_\theta/\partial J_{r0} & \partial v_\theta/\partial p_\theta \end{bmatrix}. \tag{22}$$

As the radial corrections $\hat{f}_e^{+}$ and $\hat{f}_e^{-}$ are unknown, they will be dropped from the integrals together with any other ε-order terms, and the resulting moments will have an accuracy of zeroth-order in ε in general. Of particular interest are the electron moments at the axis of the plume, $r = 0$. This is a singular line in cylindrical coordinates, as the θ direction and the v_r, v_θ velocity components are not well defined there. Special care should be used when computing moments at the axis, whether by taking the limit $r \to 0^+$ in the expressions above, or by first transforming into Cartesian coordinates before posing the moment integral to be solved. Axisymmetry considerations imply that at $r = 0$, $f_e(z, r, \theta, v_z, v_r, v_\theta)$ is symmetric in v_r and v_θ, and moreover, $f_e(z, r, \theta, v_z, v_r, v_\theta) = f_e(z, r, \theta, v_z, v_\theta, v_r)$ (i.e., the radial and azimuthal velocities are interchangeable at the axis). Therefore, at the axis odd moments in r or θ are null and even moments in r or θ are interchangeable (e.g. $\mathcal{M}_{\theta\theta} = \mathcal{M}_{rr}$).

III. Electron expansion in a radially-parabolic electric potential

As discussed above, the full plume model must determine iteratively the potential profile together with the distribution function of ions and electrons. To illustrate the application of the kinetic electron model in a given paraxial electric potential, in this section we consider the simple case where its radial profile is parabolic, i.e., that the electric potential can be written as:

$$\phi\left(z,r\right)=-\frac{ar^2}{h^2\left(\varepsilon z\right)}+\phi_1\left(\varepsilon z\right), \tag{23}$$

with a a constant that defines the the radial profile, $h\left(0\right)=1$, and $\phi_1\left(0\right)=0$. This functional form has similar mathematical properties to those expected in an actual plasma plume. Under this potential, the Hamiltonian of a single electron is

$$\mathcal{H}\left(z,r,p_z,p_r;p_\theta\right)=\frac{1}{2m_e}\left(p_z^2+p_r^2+\frac{p_\theta^2}{r^2}\right)+e\frac{ar^2}{h^2\left(\varepsilon z\right)}-e\phi_1\left(\varepsilon z\right)=E. \tag{24}$$

Observe that for $z=$ const this is the Hamiltonian of a 2D, isotropic harmonic oscillator, which can be trivially solved in Cartesian coordinates. However, we shall work in the r,θ coordinates to benefit from the conservation of p_θ. The integral for J_{r0} can in this case be solved analytically:

$$\frac{J_{r0}}{\pi}=\sqrt{\frac{m_e}{2ea}}\left[E+e\phi_1\left(\varepsilon z\right)-\frac{p_z^2}{2m_e}\right]h\left(\varepsilon z\right)-\left|p_\theta\right|. \tag{25}$$

This expression in combination with Eq. (24) can be used to write p_r as a function of z, r, J_{r0}, and p_θ:

$$\frac{1}{2m_e}p_r^2=\sqrt{\frac{2ea}{m_e}}\frac{J_{r0}/\pi+\left|p_\theta\right|}{h(\varepsilon z)}-\frac{1}{2m_e}\frac{p_\theta^2}{r^2}-e\frac{ar^2}{h^2\left(\varepsilon z\right)}, \tag{26}$$

and this result can be used to solve the integral for β_{r0} analytically:

$$\cos\left(2\pi\beta_{r0}\right)=\frac{J_{r0}/\pi+\left|p_\theta\right|-\sqrt{2eam_e}r^2/h(\varepsilon z)}{\sqrt{J_{r0}^2/\pi^2+2J_{r0}|p\theta|/\pi}}. \tag{27}$$

Observe that Eq. (25) can also be used to write E as a function of z,p_z (or equivalently, v_z), J_{r0} and p_θ.

$$E=\frac{1}{2}m_ev_z^2+U(z,J_{r0},p_\theta), \tag{28}$$

where $U(z;J_{r0},p_\theta)$ is an "effective potential" for the axial motion of the electron, which describes the confining effect of the electric potential and the accelerating effect of the conservation of J_{r0} and p_θ:

$$U(z;J_{r0},p_\theta)=-e\phi_1(\varepsilon z)+\sqrt{\frac{2ea}{m_e}}\frac{J_{r0}/\pi+\left|p_\theta\right|}{h(\varepsilon z)}. \tag{29}$$

Note that in this particular case J_{r0} and p_θ play a similar role on the axial dynamics, as they only appear through the sum $J_{r0}/\pi+|p_\theta|$ in the former equation. Incidentally, this also indicates that the frequencies of the θ and β_{r0} motions coincide, as expected in a 2D, isotropic harmonic oscillator, a fact known as a system degeneracy.[46]

The results above are valid whenever the radial potential profile is parabolic, as we have not yet decided on the form of the h and ϕ_1 functions. For the purpose of illustration of the electron dynamics only, the following functions will be used in this section:

$$h=1+\varepsilon z;\quad \phi_1=-\frac{\left|\phi_\infty\right|}{2}\left(1+\cos\frac{\pi}{1+\varepsilon z}\right). \tag{30}$$

The different phase space regions for the resulting effective potential U are plotted in Figure 2 as a function of z and E for three example values of $J_{r0}/\pi+|p_\theta|$. Imposing $v_z=0$, Eq. (28) gives the minimum energy required for the existence of an electron solution at each axial position. Interestingly, the shape of $U(z;J_{r0},p_\theta)$ for fixed J_{r0} and p_θ, and in particular its monotonicity, are determinant for the configuration of the different regions in phase space:

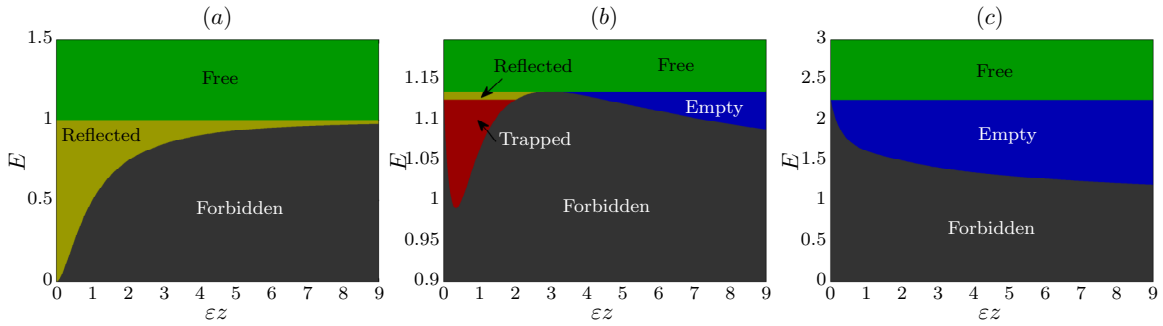

Figure 2. Energy diagrams for electrons with different values of $J_{r0}/\pi + |p_\theta|$, based on the h and ϕ_1 functions given in Equation (30). The graphs have been normalized so that $|\phi_\infty|, e, a, m_e = 1$, and plot ($a$) has $J_{r0}/\pi + |p_\theta| = 0$, plot ($b$) 2.5, and plot ($c$) 5. The color code for the different regions of phase space is as follows: grey denotes the forbidden region ($E < U$); yellow is for reflected electrons; red for doubly-trapped regions; blue for "empty" regions connecting only with infinity downstream; and green is for free, passing electrons.

- Those electrons with an energy larger than $\max(U)$ are free electrons connecting the plasma thruster ($z = 0$) with $z = \infty$ for those J_{r0} and p_θ.
- Electrons emitted at the source with an energy lower than this will be reflected when they reach the effective potential barrier (i.e., the $v_z = 0$ surface). Reflected electrons exist for that J_{r0}, p_θ pair whenever the function U has a global maximum larger than $U(0; J_{r0}, p_\theta)$.
- When the effective potential has a local minimum smaller than $U(0; J_{r0}, p_\theta)$, a region of doubly-trapped electrons exist that does not connect to either boundary of the domain.
- If the effective potential U decreases downstream with z, a last region exists which is normally empty, as it only connects with $z = \infty$. Only in the case that electrons are streaming upstream from the background would this region be populated. This region exists for large enough values of $J_{r0}/\pi + |p_\theta|$.

To further illustrate how the electron model works, we now assume f_e^+ at $z = 0$ is a monoenergetic distribution function with $E = E_1$ for all radii from $r = 0$ to $r = r^*$ (with r^* given by the condition $E_1 = -e\phi(0, r^*)$). Obviously, this is a half sphere in velocity-based phase space, with a radius that depends linearly on r. It can be shown that this distribution function has $\overline{f}_e^+ \equiv f_e^+$ and $\hat{f}_e^+ = 0$. The same distribution function in energy-based phase space is a double triangular sheet in the $E = E_1$ plane, as shown in Fig. 3.

It is worth noting that this single figure in energy-based space is a compact representation of the f_e^+ distribution function at all radii of the $z = 0$ plane. Indeed, since this distribution function is uniform in β_{r0}, each point within the double-triangle represents a complete radial electron orbit, with its own turning points $r_{\min}$ and $r_{\max}$ where the radial velocity $v_r(z, r, J_{r0}, p_\theta)$ cancels out (equivalently, $p_r = 0$ in Eq. (26)). At each radial position r, only a subset of all the possible radial orbits contribute to the distribution function there, the condition being $r_{\min} \leq r \leq r_{\max}$. The boundary where $v_r = 0$ that delimits that subset is a parabola (as can be inferred from Eq. (26)) and has been plotted on top of Fig. 3 for several radii. At the axis, only the electrons with $p_\theta = 0$ contribute to the distribution function there. Particles with $J_{r0} = 0$ have $r_{\min} = r_{\max}$ and only contribute to f_e^+ at a single value of r.

The solution procedure described in the previous section can be applied to this boundary condition for f_e^+ at $z = 0$ in the radially-parabolic potential of Eq. (23). Assuming $f_e^- = 0$ at $z \to \infty$, the method of characteristic allows the direct computation of $\overline{f}_e$ at all values of z. The resulting distribution function is plotted in Fig. 4 for an energy E_1 slightly larger than $|\phi_\infty|$ to illustrate all the different region types. Initially, only free and reflected electrons exist; in the reflected region, $f_e^- = f_e^+$. A bit further downstream, doubly-trapped electrons exist. This population decreases as z increases and eventually disappears. The same fate reaches the reflected population as the maximum in the effective potential U is reached. After that point, only the free electrons (whose region obviously remains immutable in the whole domain) exist. Finally a new region of existence opens up, connected only to the downstream boundary condition and therefore empty in this example.

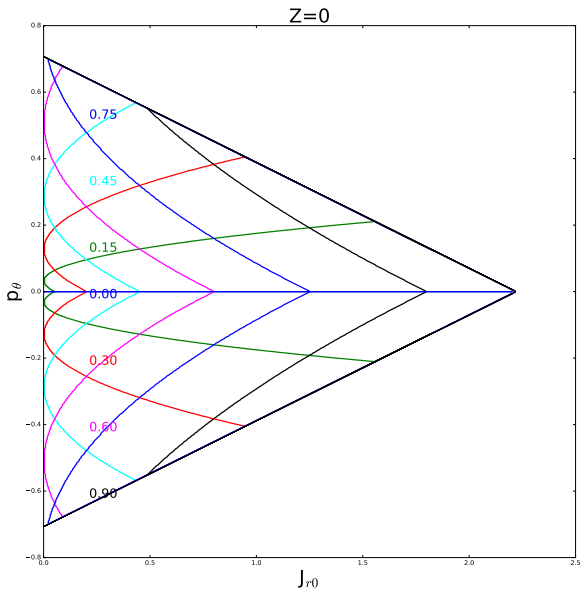

Figure 3. Representation of a f_e^+ monoenergetic distribution function for all radii in the radially-parabolic potential field at $z = 0$, with normalized variables $E_1, e, a, m_e = 1$. The colored lines indicate the boundary of the regions of the figure that contribute to the distribution function at one radius r as labeled.

IV. Toward a full plasma plume model

In the previous sections, a kinetic electron model that takes a prescribed electric potential as an input has been formulated. The solution procedure has been illustrated for a simple case. As stated in the introduction, this electron model is the main ingredient for a full plasma plume model that solves the ion and electron distribution functions together with the electric potential. In this section, we discuss the minimal additional parts of a full model that need to be developed in order to complete the description of the problem.

A. Ion model

While electrons are radially confined by the electric field and most of the population completes several radial orbits before experiencing substantial axial motion, all ions are accelerated outward by the electric field. As they are not confined by the electric potential and do not have substantial radial motion, the model derived above for electrons based on the quasi-conservation of the integral J_{r0} is inadequate for the ion population. Since we are mainly interested in obtaining the self-consistent plasma plume response to study the electron behavior and not so much the ion properties, we only require the ion density for a prescribed electric potential as output from the ion model, in order to be able to set up an iterative procedure toward the full solution.

The primary ions coming out from the thruster are typically nearly-cold compared to the electrons,

$$T_i \ll T_e, \tag{31}$$

and their temperature T_i may be neglected in first approximation. Moreover, primary ions are commonly also hypersonic, i.e., the ion Mach number $M = u_i/c_s$ is much larger than unity (where u_i is the ion fluid velocity and c_s is the sound velocity in the plasma); in other words,

$$\frac{u_i}{\sqrt{T_e/m_i}} \gg 1. \tag{32}$$

The motion of the population is simple enough to be solved by direct numerical simulation in the 2D domain. This can be approached by direct integration of the trajectories of representative ions born at the $z = 0$

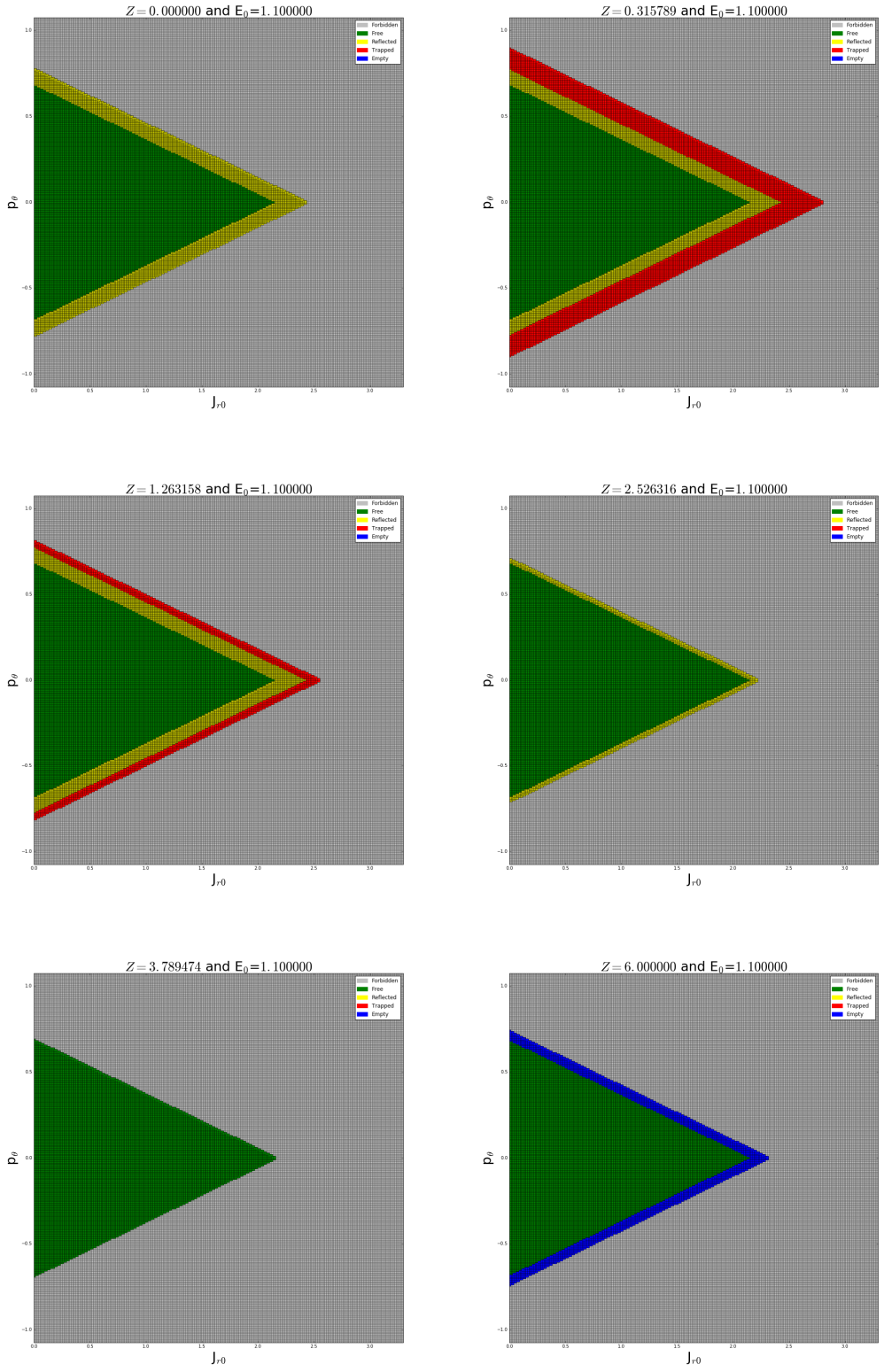

Figure 4. Solution of the distribution function $\overline{f}_e$ in the radially-parabolic potential at various axial positions, for f_e^+ at $z = 0$ a monoenergetic distribution function of the type depicted in Fig. 3 and $f_e^- = 0$ at $z \to \infty$. The normalized variables $|\phi_\infty|, e, a, m_e = 1$ and $E_1 = 1.1$ have been used. The color code for the different regions is the same as in Fig. 2.

plane, or (equivalently) by solving the fluid continuity and momentum equations of cold ions. Either way, the conservation of E and p_θ of ions can be used to further simplify the solution procedure. More advanced primary ion models, e.g. relaxing the 'cold ion' hypothesis, could be considered as extensions of this first version of the model.

Secondary ions, i.e. those formed outside of the thruster by e.g. charge-exchange collisions, constitute a low-density population that does not strongly influence the electric potential in the plume, which is dominantly set up by the electrons and the primary ions. As such, secondary electrons can be neglected in first approximation when the goal is to obtain the self-consistent electric potential and study the collisionless electron cooling mechanisms in the plume (especially its far-region, as secondary ion density drops quickly downstream).

B. Iteraterative calculation of the self-consistent electric potential

With the models above, it is possible to compute the ion and electron moments anywhere in the 2D plume for an assumed electric potential. However, we still lack a procedure to obtain the self-consistent electric potential of the plasma plume, which must result from the charge balance between ions and electrons. Assuming an initial guess for ϕ, the ion and electron densities can be calculated. Then, Poisson's equation can be used to compute a new potential and iterate on, until the error in the 2D plume is as low as desired. Alternatively, the quasineutrality assumption can be invoked and the difference between ion and electron densities used as the error metric to set up the iterative procedure.

In summary, the following iterative procedure can be used to solve the 2D plume model, starting from an approximate electric potential such as that given by the EASYPLUME code:[30]

1. Given the electric potential $\phi(z,r)$ and the boundary conditions f_e^+ at $z=0$ and f_e^- at $z\to\infty$, we compute the density $n_e(z,r)$ with the kinetic electron model and $n_i(z,r)$ with direct integration of the cold ion fluid equations over a predefined grid.

2. We compute the new $\phi(z,r)$ using Poisson's equation (alternatively, quasineutrality is used to compute the error committed and recompute the new potential)

3. The procedure is repeated until the error is smaller than a predefined tolerance and convergence is achieved.

Instead of solving the full 2D problem, a simplification can be called forth to establish a quasi-1D model, by first establishing a quasi-separable functional form for the electric potential and fixing the radial dependency of ϕ. This approximation is consistent with self-similar fluid models, which have been successfully used to accurately describe laboratory and in-space plumes.[6]

In the case of a functional form such as that of Eq. (10), function ϕ_0 would be prescribed *a priori* based on e.g. experimental knowledge of this profile at a particular $z=$ const plane. Then, the iterative procedure would merely solve for the ϕ_1 and h functions, considering only the error at the axis (or alternatively the average error for all r). This quasi-1D is deemed more accessible for the first version of the complete model, and is expected to yield reasonably accurate results in the full 2D domain.

To conclude this section, it is noted that we have implicitly assumed that a steady-state solution for the plasma plume exists and is unique. Even if we accept that this is physically the case, the consistency, convergence and stability of the iterative method have to be assessed.

V. Conclusion

A kinetic electron model for collisionless electrons in a paraxial plasma plume has been presented which makes use of the near-conservation of the radial-motion action integral to reduce the determination of the electron distribution function in the domain to a trivial propagation problem in the axial direction. The radially-averaged distribution function can be determined with an error of order $O(\varepsilon^2)$, where ε is the small parameter associated to paraxiality. The error of the computed distribution moments is in general of order $O(\varepsilon)$.

Electrons are nearly confined by the electric field in the plume, and their high mobility in the near-collisionless plasma results in an electron response that is *global* in its nature. The combined effect of the electric potential and the conservation of the adiabatic invariants of the electron motion results in an electron

phase space divided into free electrons, reflected electrons, doubly-trapped electrons, and empty regions (or regions filled with a downstream electron population). The different regions have been illustrated for an assumed electric potential profile that is radially-parabolic. The present model allows "filling" the doubly-trapped regions with an arbitrary distribution function, and the upstream distribution (or a fraction of it) is proposed as the simplest option. Future work must consider the transient expansion of the plume and other effects like weak collisionality and higher order terms to study the electron distribution function in those regions. An example based on a monoenergetic boundary condition upstream has been used to illustrate the functioning of the model. The validity of the model assumptions and the conservation of J_{r0} shall be investigated in more detail as a next step with a simple particle code.

The electron model can be used in conjunction with an ion model to determine iteratively the self-consistent plasma and electric potential solutions. A 2D and a quasi-1D procedure based on solving Poisson's equation or enforcing quasineutrality has been proposed and will be object of future work. The intended application of such model is to study the evolution of several electron moments (in particular, the components of the temperature tensor and heat fluxes) along the plasma plume, and the collisionless cooling mechanisms that may exist. The resulting 'cooling laws' may then be employed as an improvement over the extensively used isothermal or polytropic models commonly implemented in multi-fluid and PIC/fluid plasma plume codes.

Acknowledgments

The authors would like to thank Jesus Ramos and Manuel Martínez-Sánchez from MIT for the insightful discussions. This work has been supported by ESA project 4000116180/15/NL/PS, "Model and experimental validation of spacecraft-thruster interactions (erosion) for electric propulsion thruster plumes." Additional support came from the Spanish R&D National Plan, grant number ESP2013-41052-P. Aurélien Proux's work has been supported by the Erasmus+ internship program.

References

[1]Jahn, R., *Physics of Electric Propulsion*, Dover, 2006.

[2]Goebel, D. M. and Katz, I., *Fundamentals of Electric Propulsion: Ion and Hall Thrusters*, JPL, 2008.

[3]Kaufman, H., "Interaction of a solar array with an ion thruster due to the charge-exchange plasma. NASA report CR-135099," Tech. rep., NASA Lewis Research Center, 1976.

[4]Boyd, I. and Ketsdever, A., "Interactions between spacecraft and thruster plumes," *Journal of Spacecraft and Rockets*, Vol. 38, No. 3, 2001, pp. 380.

[5]Ferguson, D. and Hillard, G., "Low Earth orbit spacecraft charging design guidelines," *NASA Marshall Space Flight Center, Huntsville, AL, NASA TP-2003-212287*, 2003.

[6]Korsun, A., Tverdokhlebova, E., and Gabdullin, F., "The Distinction between the EP Plume Expansion in Space and in Vacuum Chamber," *Proceedings of the 29th International Electric Propulsion Conference*, 2005, pp. 05–0073.

[7]Wartelski, M., Theroude, C., Ardura, C., and Gengembre, E., "Self-consistent Simulations of Interactions between Spacecraft and Plumes of Electric Thrusters," *33rd International Electric Propulsion Conference*, No. IEPC-2013-73, 2013.

[8]Merino, M., Ahedo, E., Bombardelli, C., Urrutxua, H., and Peláez, J., "Ion Beam Shepherd satellite for Space Debris Removal," *Progress in Propulsion Physics*, edited by L. T. DeLuca, C. Bonnal, O. J. Haidn, and S. M. Frolov, Vol. IV of *EUCASS Advances in Aerospace Sciences*, chap. 8, Torus Press, 2013, pp. 789–802.

[9]Bombardelli, C., Urrutxua, H., Merino, M., Ahedo, E., and Peláez, J., "The ion beam shepherd: A new concept for asteroid deflection," *AA*, Vol. 90, No. 1, 2013, pp. 98 – 102.

[10]Myers, R. and Manzella, D., "Stationary Plasma Trhuster Plume Characteristics," *23rd International Electric Propulsion Conference, Seattle, WA*, IEPC 93-096, 1993.

[11]Haas, J. M. and Gallimore, A. D., "An Investigation of Internal Ion Number Density and Electron Temperature Profiles in a Laboratory-Model Hall Thruster," *36th AIAA/ASME/SAE/ASEE Joint Propulsion Conference & Exhibit*, AIAA, Washington DC, 2000.

[12]Manzella, D., Jankovsky, R., Elliott, F., Mikellides, I., Jongeward, G., and Allen, D., "Hall Thruster Plume Measurements On-board the Russian Express Satellites. NASA report TM-2001-211217," Tech. rep., 2001.

[13]Beal, B., Gallimore, A., and W.A. Hargus, J. H., "Plasma Properties in the Plume of a Hall Thruster Cluster," *Journal of Propulsion and Power*, Vol. 20, No. 20, 2004, pp. 985 – 991.

[14]Ekholm, J. M., Hargus, W. A., Larson, C. W., Nakles, M. R., Reed, G., and Niemela, C. S., "Plume characteristics of the busek 600 w Hall thruster," *Proceedings of the 42nd Joint Propulsion Conference and Exhibit*, No. AIAA-2006-4659, 2006.

[15]L. Brieda, M. N., D. R. Garrett, W. J. H., and Randy, R., "Experimental and Numerical Examination of the BHT-200 Hall Thruster Plume," *43rd AIAA/ASME/SAE/ASEE Joint Propulsion Conference & Exhibit*, AIAA, Washington DC, 2007.

[16]Dannenmayer, K., Mazouffre, S., Ahedo, E., and Merino, M., "Hall Effect Thruster Plasma Plume Characterization with Probe Measurements and Self-Similar Fluid Models," *48th AIAA/ASME/SAE/ASEE Joint Propulsion Conference & Exhibit*, No. AIAA 2012-4117, AIAA, Atlanta, Georgia, 2012.

[17]Aston, G., Kaufman, H., and Wilbur, P., "Ion beam divergence characteristics of two-grid accelerator systems," *AIAA Journal*, Vol. 16, 1978, pp. 516–524.

[18]Takegahara, H., Kasai, Y., Gotoh, Y., Miyazaki, K., Hayakawa, Y., Kitamura, S., Nagano, H., and Nanamura, K., "Beam characteristics evaluation of ETS-VI Xenon ion thruster," *23rd International Electric Propulsion Conference*, No. IEPC-93-235, 1993.

[19]Foster, J., Soulas, G., and Patterson, M., "Plume and discharge plasma measurements of an NSTAR-type ion thruster," *36th Joint Propulsion Conference and Exhibit, Huntsville, Alabama*, 2000.

[20]Pollard, J., "Plume Angular, Energy, and Mass Spectral Measurements with the T5 Ion Engine," *Proceedings of the 31st Joint Propulsion Conference and Exhibit*, No. AIAA-95-2920, 1995.

[21]Kamhawi, H., Soulas, G., Patterson, M., and Frandina, M., "NEXT ion engine 2000 hour wear test plume and erosion results," *AIAA Paper*, Vol. 3792, 2004.

[22]Azziz, Y., *Experimental and Theoretical Characterization of a Hall Thruster Plume*, Ph.D. thesis, Massachusetts Institute of Technology, 2007.

[23]Wang, J., Brinza, D., Goldstein, R., Polk, J., Henry, M., Young, D., Hanley, J., Nordholt, J., Lawrence, D., and Shappirio, M., "Deep Space One Investigations of Ion Propulsion Plasma Interactions: Overview and Initial Results," *AIAA Paper*, Vol. 2971, 1999.

[24]Brinza, D., Wang, J., Polk, J., and Henry, M., "Deep Space 1 measurements of ion propulsion contamination," *J. Spacecraft & Rockets*, Vol. 38, No. 3, 2001.

[25]Hilgers, A., Thiébault, B., Estublier, D. L., Gengembre, E., Del Amo, J. G., Capacci, M., Roussel, J., Tajmar, M., and Forest, J., "A simple model of the effect of solar array orientation on SMART-1 floating potential," *IEEE transactions on plasma science*, Vol. 34, No. 5, 2006, pp. 2159.

[26]Estublier, D. L., "The SMART-1 spacecraft potential investigations," *IEEE Transactions on Plasma Science*, Vol. 36, No. 5, 2008, pp. 2262–2270.

[27]Parks, D. and Katz, I., "A preliminary model of ion beam neutralization," *14th International Electric Propulsion Conference*, Electric Rocket Propulsion Society, Fairview Park, OH, 1979.

[28]Korsun, A. and Tverdokhlebova, E., "The characteristics of the EP exhaust plume in space," *33rd AIAA/ASME/SAE/ASEE Joint Propulsion Conference & Exhibit*, AIAA, Washington DC, 1997.

[29]Ashkenazy, J. and Fruchtman, A., "Plasma plume far field analysis," *27th International Electric Propulsion Conference*, Electric Rocket Propulsion Society, Fairview Park, OH, 2001.

[30]Merino, M., Cichocki, F., and Ahedo, E., "Collisionless Plasma thruster plume expansion model," *Plasma Sources Science and Technology*, Vol. 24, No. 3, 2015, pp. 035006.

[31]Cichocki, F., Merino, M., Ahedo, E., Hu, Y., and Wang, J., "Fluid vs PIC Modeling of a Plasma Plume Expansion," 34^{th} *International Electric Propulsion Conference*, No. IEPC-2015-420, Electric Rocket Propulsion Society, Fairview Park, OH, 2015.

[32]Wang, J., Brinza, D., and Young, M., "Three-Dimensional Particle Simulation Modeling of Ion Propulsion Plasma Environment for Deep Space One," *Journal of Spacecraft and Rockets*, , No. 3, 2001.

[33]Hu, Y. and Wang, J., "Electron Properties in Collisionless Mesothermal Plasma Expansion: Fully Kinetic Simulations," *Plasma Science, IEEE Transactions on*, Vol. 43, No. 9, 2015, pp. 2832–2838.

[34]Boyd, I. and Dressler, R., "Far field modeling of the plasma plume of a Hall thruster," *Journal of applied physics*, Vol. 92, No. 4, 2002, pp. 1764.

[35]Santi, M., Cheng, S., Celik, M., Martínez-Sánchez, M., and Peraire, J., "Further development and preliminary results of the AQUILA Hall thruster plume model," *39th Joint Propulsion Conference, Huntsville, AL*, 2003.

[36]Brieda, L., Kafafy, R., Pierru, J., and Wang, J., "Development of the draco code for modeling electric propulsion plume interactions," *Proceedings of the 40th Joint Propulsion Conference, Fort Laudardale, FL, USA*, 2004, pp. 1–21.

[37]Araki, S. J., Martin, R. S., Bilyeu, D., and Koo, J. W., "SM/MURF: Current Capabilities and Verification as a Replacement of AFRL Plume Simulation Tool COLISEUM," *52nd AIAA/SAE/ASEE Joint Propulsion Conference*, 2016, p. 4939.

[38]Roussel, J.-F., Rogier, F., Dufour, G., Mateo-Velez, J.-C., Forest, J., Hilgers, A., Rodgers, D., Girard, L., and Payan, D., "SPIS open-source code: Methods, capabilities, achievements, and prospects," *IEEE Transactions on Plasma Science*, Vol. 36, No. 5, 2008, pp. 2360–2368.

[39]Cichocki, F., Merino, A. D., and Ahedo, E., "A 3D hybrid code to study electric thruster plumes," *Space Propulsion Conference 2016*, No. 3124968, European Space Agency, Rome, Italy, 2016.

[40]Navarro, J., Martinez-Sanchez, M., and Ahedo, E., "Collisionless electron cooling in a magnetic nozzle," *50th AIAA/ASME/SAE/ASEE Joint Propulsion Conference*, AIAA, Cleveland, Ohio, 2014.

[41]Martinez-Sanchez, M., Navarro-Cavallé, J., and Ahedo, E., "Electron cooling and finite potential drop in a magnetized plasma expansion," *Physics of Plasmas*, Vol. 22, No. 5, 2015, pp. 053501.

[42]Andersen, S., Jensen, V., Nielsen, P., and D'Angelo, N., "Continuous Supersonic Plasma Wind Tunnel," *Phys. Fluids*, Vol. 12, No. 3, 1969, pp. 557–560.

[43]Ahedo, E. and Merino, M., "Two-dimensional supersonic plasma acceleration in a magnetic nozzle," *Physics of Plasmas*, Vol. 17, 2010, pp. 073501.

[44]Arefiev, A. and Breizman, B., "Ambipolar acceleration of ions in a magnetic nozzle," *Physics of Plasmas*, Vol. 15, No. 4, 2008, pp. 042109.

[45]Martínez-Sánchez, M. and Ahedo, E., "Magnetic Mirror Effects on a Collisionless Plasma in a Convergent Geometry," *Physics of Plasmas*, Vol. 18, 2011.

[46]Goldstein, H., Poole, C., and Safko, J., *Classical mechanics*, Addison Wesley, 2001.